

Thermodynamics of first-order and continuous melting of xenon on graphite

N. J. Colella and R. M. Suter

*Department of Physics and Center for the Study of Materials,
Carnegie-Mellon University, Pittsburgh, Pennsylvania 15213*

(Received 15 April 1986)

We report a high-precision vapor-pressure isotherm study of the melting of near-monolayer xenon adsorbed on Union Carbide's ZYX exfoliated graphite. The data are analyzed in terms of the film isothermal compressibility K_T . We identify a sharp peak in K_T which occurs in low-temperature data as a first-order melting transition. As the temperature is increased, the amplitude of the peak decreases, reaching zero at a tricritical temperature $T_i = 147 \pm 4$ K. Above this temperature the melting appears to be continuous. A temperature-independent, weak, and relatively broad contribution to K_T underlies the sharp peak at low T and persists above T_i ; we discuss possible origins of this component.

The melting of near-monolayer Xe on graphite is one of the most thoroughly studied realizations of a two-dimensional melting transition.¹ The Xe atoms form an ordered phase which is incommensurate with the underlying graphite and has a power-law structure factor.^{2,3} The system is, therefore, a candidate for testing the dislocation mediated continuous melting theory of Kosterlitz and Thouless, Nelson and Halperin, and Young (KTNHY).⁴ Extensive high-resolution synchrotron x-ray scattering studies^{2,3} using high-quality substrates (Union Carbide's ZYX exfoliated graphite and, recently, a single crystal) indicate a continuous transition at temperatures above 125 K and a weak first-order transition below this temperature. Heat-capacity measurements⁵ on Grafoil show weak, broad peaks which have been interpreted as indicating continuous transitions for $T \geq 106$ K. A vapor-pressure isotherm (VPI) study,⁶ on the other hand, shows no resolved change in isotherm shape from 110 to nearly 150 K; the authors estimate a tricritical temperature between 150 and 160 K. We have performed a new VPI study using a ZYX substrate; we deduce the isothermal compressibility of the film through numerical differentiation of the data and we are thus able to resolve new details of the melting-transition thermodynamics.

EXPERIMENT

Our data are qualitatively similar to the results of previous isotherm measurements of Xe melting on graphite,^{6,7} but we probe the transition region on a fine grid and use an extremely careful equilibration procedure. Our substrate, apparatus, and procedure are the same as those used in work on the Kr/graphite system.⁸ We use ZYX graphite as substrate since it has the highest surface coherence length of the available exfoliates⁹ and is known to have a highly homogeneous adsorption potential.⁸ In the temperature range studied, the transition vapor pressure varies by a factor of a thousand, so we use three different MKS Baratron pressure gauges, with 1, 10, and 100 Torr full scales.

In the following, all our results are reported in terms of the film chemical potential, in Kelvin units, and tempera-

ture. We convert from three-dimensional vapor pressure to the chemical potential of the vapor (and thus also the film) using the ideal-gas formula. The use of the thermodynamic variables of the film itself allows us to directly compare widths and shapes of data at different temperatures. We calculate the quantity $K_T = n^{-2} \partial n / \partial \mu$, where n is the surface coverage in monolayer units and μ is the chemical potential, by taking differences between neighboring data points without numerical smoothing. K_T is proportional to the film isothermal compressibility. To determine the maximum monolayer coverage, we have taken isotherms which extend into the second layer region at 105.5, 145, 148.2, 150, and 152.1 K.¹⁰ We take the formation of a second layer gas to be indicated by a statistically significant increase in the effective compressibility above its minimum value in the monolayer solid phase. The coverage at which this occurs is found to be independent of temperature to about 3% accuracy; we chose this coverage, 5.55×10^{14} cm⁻², as our definition of one monolayer (ML). The traditional Thomy and Duval⁷ definition would yield an ML density 12% less than ours.

Before presenting our data, we summarize the functional forms expected in the VPI near the melting transition. For an ideal system, in a first-order coexistence region one expects an increase in coverage at fixed chemical potential; thus, K_T contains a δ -function singularity. In the case of a KTNHY transition, at most a smooth, nonsingular anomaly is expected in K_T ; the isotherm should also contain at most a smooth anomaly. Real substrates are composed of finite-sized crystallites and have some heterogeneity in the adsorption potential. These effects lead to rounding of any sharp features in the ideal system.^{11,12} For Kr adsorption on our substrate, we previously found⁸ a 2-K-wide chemical potential smearing of an apparently first-order transition. We expect inhomogeneities in the Xe adsorption case to be of the same order, perhaps being scaled up by the stronger adsorption potential to as much as 3 K. This is comparable to estimates by Ecke, Dash, and Puff¹² for the heterogeneity of Xe on an uncompressed exfoliated graphite. Near a KTNHY transition, the compressibility anomaly will be essentially undistorted by inhomogeneities if it is considerably broader than the 2–3-K substrate reso-

lution. On the other hand, near such a transition the correlation length becomes large and finite-size effects limit the observation of truly asymptotic behavior.^{2,3}

RESULTS

Figure 1(a) shows three isotherms in the vicinity of the melting transition. The data are plotted against chemical potential difference from the point of maximum slope. The figure illustrates that with increasing temperature the transition density gradually increases, at an approximately constant 0.003 ML/K, while the density difference between liquid ($\Delta\mu < 0$) and solid ($\Delta\mu > 0$) phases decreases. It is also apparent that the maximum slope achieved by the data decreases as the temperature is raised.¹³ K_T , shown in Fig. 1(b), provides a more dramatic illustration of the similarities and distinctions among the data sets. Note that the vertical scale is logarithmic: The peak compressibility at 116 K is about six times that at 145 K. Three chemical potential regions should be noted.

(i) The only strongly temperature-dependent part of the compressibility is seen in an extremely narrow region: $|\Delta\mu| \leq 1$ K. For temperatures less than $T_i = 147 \pm 4$ K, K_T in this region contains a peak which extends above a

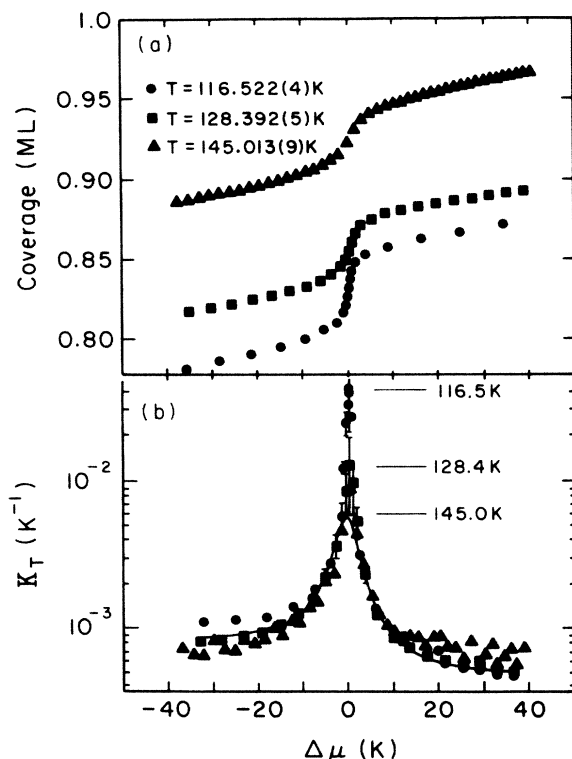


FIG. 1. (a) Vapor-pressure isotherms in the liquid-solid transition region plotted in monolayer units against chemical potential deviation from the point of maximum slope. Transition vapor pressures for these three runs, in order of ascending temperature, are 0.0374, 0.5834, and 14.65 Torr. (b) Isothermal compressibilities deduced from the isotherms in (a) as described in the text. For clarity, the labeled horizontal lines mark the peak value achieved by each of the data sets. The solid line is a Lorentzian least-squares fit to the 128.4-K data.

broad contribution (described below), whereas for $T > T_i$, no central peak is observed. With decreasing temperature, this sharp peak grows in height until it becomes almost an order of magnitude larger than the broad component. The chemical potential width of this contribution appears to be temperature independent.

(ii) In the region $1 < |\Delta\mu| < 20$ K the compressibility is, to a startling degree, independent of temperature. K_T rises almost an order of magnitude above the background, but is quite weak compared to the sharp central peak seen in the lower-temperature data. The width of this weak component is large compared to expected heterogeneous smearing of a first-order transition.

(iii) Far from the peak, the compressibility approaches an approximately constant value for each isotherm. The solid-phase compressibility at $\Delta\mu = +40$ K is nearly temperature independent and the liquid-phase value at $\Delta\mu = -40$ K decreases with increasing temperature until it becomes equal to that of the solid near $T = 147$ K.

The above empirical separation of the chemical potential dependence of the anomaly in K_T into two components is made possible only by the distinctly different temperature dependencies: The sharp component has a strong dependence, while the weaker and broader component is essentially independent of temperature. To quantify the degree of temperature dependence of the weak anomaly, we have fit our data in the range $1 < |\Delta\mu| < 40$ K to a Lorentzian plus independently determined backgrounds on the liquid and solid sides; the Lorentzian form was chosen simply because, to the precision of our data, it adequately parametrizes the observed shape. The fit to the data at 128.4 K is shown in Fig. 1(b). In Fig. 2, the fitting is

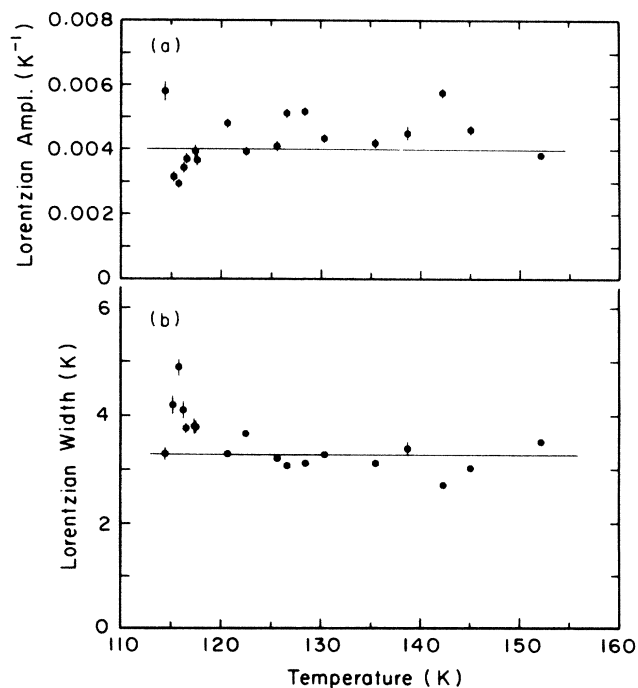


FIG. 2. Results of Lorentzian least-squares fits of the compressibilities in the region $1 < |\Delta\mu| < 40$ K. (a) Lorentzian amplitude and (b) Lorentzian half width at half maximum. Weighted means are given by the solid lines.

shown to yield amplitudes of $4.0 \pm 0.4 \times 10^{-3} \text{ K}^{-1}$ and half widths at half maximum in the range $3.3 \pm 0.1 \text{ K}$ in chemical potential, with no apparent variation with temperature. It is difficult to see how the entire compressibility anomaly can be due to a single physical mechanism. For a strong first-order or a continuous transition, one would expect, even in the presence of inhomogeneities, that the entire anomaly would scale in a consistent way as the phase boundary is crossed at different temperatures. As detailed below, we believe that the composite behavior can be described by a weak first-order transition which is preceded by precursive critical behavior.

We take the sharp peak in K_T to indicate a substrate limited first-order transition. As the temperature is raised, this peak becomes weaker and only the broad, weak anomaly is left at $T \geq 147 \pm 4 \text{ K}$. Thus, the density width of the liquid-solid coexistence region decreases to below our resolution ($\sim 0.001 \text{ ML}$) near this temperature and the melting transition is apparently continuous for higher temperatures. For $T \geq 147 \text{ K}$ the lack of apparent singular behavior in the thermodynamic response, combined with x-ray scattering data^{2,3} demonstrating a divergence in the density-density correlation length, is consistent with a dislocation unbinding melting transition as envisioned by KTNHY.⁴ Unfortunately, our present data do not extend far into the continuous region due to our decreased resolution as the transition vapor-pressure increases exponentially.^{6,7} However, as demonstrated in Fig. 2, the nonsingular anomaly which remains at temperatures as high as 152 K has a shape which is indistinguishable from that which underlies the sharp first order component at low temperatures.

In the first-order region, the temperature dependence of the coverage difference between coexisting liquid and solid phases can be deduced from our data. The density width cannot, however, simply be read off the isotherm since, in

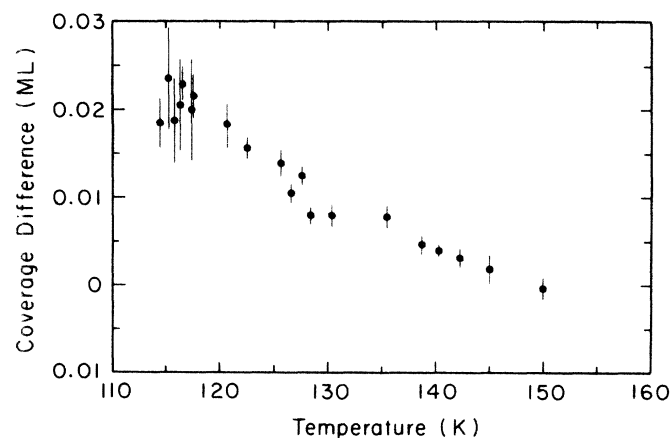


FIG. 3. Variation with temperature of the coverage (or density) difference between coexisting liquid and solid phases. Note the zero offset of the vertical scale. Below 120 K , errors are primarily due to uncertainty in the absolute transition vapor pressure, while at higher temperatures they are mainly due to interpolation uncertainty. An additional uncertainty of ± 0.002 monolayers is associated with our uncertainty in the Lorentzian amplitude.

the $\Delta\mu \sim 2 \text{ K}$ wide smearing region, a finite contribution from the broad, weak anomaly would also be included. We use the following procedure: We read off of the isotherm the coverage difference between $\Delta\mu = -1$ and $+1 \text{ K}$; we then subtract the coverage difference obtained by integrating the temperature independent anomaly, approximated by the weighted average of the Lorentzian parameters shown in Fig. 2, plus the uniform phase backgrounds (the amount subtracted, which can be deduced from Fig. 1 and the definition of K_T is $\sim 0.8\% \text{ ML}$). The resultant coverage differences are plotted in Fig. 3. Power-law fits to these data are extremely sensitive to uncertainties in the subtraction procedure: Exponents between 1 and 2 and T_i between 145 and 155 K can be obtained.

DISCUSSION

We conclude that the melting transition of Xe on graphite at $T > T_i$ is continuous. This conclusion is consistent with both thermodynamic and x-ray scattering data. The present work, however, is the first determination of the temperature dependence of the first order density difference near the tricritical point and is thus the clearest indication available of the change from first order to continuous melting. The scattering measurements on ZYX (Ref. 2) appear to exhibit crossover near 125 K , from weak first-order to continuous transitions. While this is $\sim 20 \text{ K}$ below our T_i the coverage difference in the intervening region is less than 1% of a monolayer. Coexistence, even at 116 K , is a subtle effect in the scattering lineshape, whereas it has a strong thermodynamic signal. It should also be pointed out that the lack of a sharp component in K_T above T_i argues against Abraham's interpretation of the x-ray data.¹⁴

We suggest two possible origins for the weak and, to our resolution, temperature-independent anomaly in K_T : Either it is a signal of the KTNHY dislocation unbinding process⁴ or it is due to the proximity of the tricritical point. In the former case, it would seem puzzling that at $T < T_i$ the first-order transition occurs in the center of the anomaly since melting is normally expected to occur on the solid side tail of the dislocation unbinding anomaly. Thus, the temperature-independent peak may be due to precursive tricritical behavior and may indicate that the tricritical compressibility is not divergent. Clearly, a theoretical treatment of tricritical crossover, including the effect of a substrate which imposes long-range orientational order, would be most helpful.

Finally, is the experimentally observed continuous melting behavior an artifact? Increased smearing at high temperatures could conceivably be generated by phase boundary bending: As a boundary becomes parallel to the thermodynamic path followed, the effects of inhomogeneities will become more dramatic.¹¹ We believe that such effects are negligible since our data indicate an essentially straight coverage-temperature phase boundary, and since we observe that both components of K_T have widths which are temperature independent. On the other hand, it is possible that the density difference, shown in Fig. 3, remains finite to higher temperatures than we have supposed. The size of such a first-order region would be exceedingly

small. We are currently extending our measurements in the tricritical region using a smaller volume gas handling system.

We thank P. Dimon, J. G. Fetkovich, R. B. Griffiths, G. Grinstein, P. M. Horn, J. Nagle, K. Strandburg, and R. H. Swendsen for helpful comments and conversa-

tions. Assistance of W. Wang in data analysis and editorial assistance from C. Nelson are gratefully acknowledged. We thank MKS Instruments for an equipment donation. Finally, we acknowledge support from the Samuel and Emma Winters Foundation and the National Science Foundation through Materials Research Laboratory Grant No. DMR 8119507.

-
- ¹For examples of other systems, see *Ordering in Two Dimensions*, edited by S. K. Sinha (North-Holland, Amsterdam, 1980).
- ²P. Dimon, P. M. Horn, M. Sutton, R. J. Birgeneau, and D. E. Moncton, *Phys. Rev. B* **31**, 437 (1984); P. A. Heiney, P. W. Stephens, R. J. Birgeneau, P. M. Horn, and D. E. Moncton, *ibid.* **28**, 6416 (1983); E. M. Hammonds, P. Heiney, P. W. Stephens, R. J. Birgeneau, and P. M. Horn, *J. Phys. C* **13**, L301 (1980).
- ³E. D. Specht, R. J. Birgeneau, K. L. D'Amico, D. E. Moncton, S. E. Nagler, and P. M. Horn (unpublished); S. E. Nagler, P. M. Horn, T. F. Rosenbaum, R. J. Birgeneau, M. Sutton, S. G. J. Mochrie, D. E. Moncton, and R. Clarke, *Phys. Rev. B* **32**, 7373 (1985); T. F. Rosenbaum, S. E. Nagler, P. M. Horn, and R. Clarke, *Phys. Rev. Lett.* **50**, 1791 (1983).
- ⁴J. M. Kosterlitz and D. J. Thouless, *J. Phys. C* **6**, 1181 (1973); J. M. Kosterlitz, *ibid.* **7**, 1046 (1974); D. R. Nelson and B. I. Halperin, *Phys. Rev. B* **19**, 2457 (1979); A. P. Young, *ibid.* **19**, 1855 (1979).
- ⁵J. A. Litzinger, Ph.D. thesis, University of Pittsburgh, 1980 (unpublished).
- ⁶C. Tessier, Ph.D. thesis, L'Universite de Nancy I, 1983.
- ⁷A. Thomy and X. Duval, *J. Chim. Phys.* **66**, 1966 (1969); **67**, 286 (1970); **67**, 1101 (1970).
- ⁸R. M. Suter, N. J. Colella, and R. Gangwar, *Phys. Rev. B* **31**, 627 (1985).
- ⁹R. J. Birgeneau, P. A. Heiney, and J. P. Pelz, *Physica B* **109 & 110**, 1785 (1982).
- ¹⁰N. J. Colella and R. M. Suter (unpublished).
- ¹¹J. G. Dash and R. D. Puff, *Phys. Rev. B* **24**, 295 (1981).
- ¹²R. E. Ecke, J. G. Dash, and R. D. Puff, *Phys. Rev. B* **26**, 1288 (1982).
- ¹³N. J. Colella and R. M. Suter, *Bull. Am. Phys. Soc.* **30**, 334 (1985).
- ¹⁴F. F. Abraham, *Phys. Rev. B* **29**, 2606 (1984); **28**, 7338 (1983); *Phys. Rev. Lett.* **50**, 978 (1983).